ELSEVIER

Journal of Organometallic Chemistry 498 (1995) 177–186

Journal of Organometallic Chemistry

Structure and catalytic activity of phosphine-substituted ruthenium carbonyl carboxylates

Ugo Matteoli [a], Gloria Menchi [b], Mario Bianchi [b], Franco Piacenti [b,*], Sandra Ianelli [c], Mario Nardelli [c]

[a] *Dipartimento di Chimica, Università di Venezia, Calle Larga S. Marta 2137, I-30123 Venice, Italy*
[b] *Dipartimento di Chimica Organica "Ugo Schiff", Università di Firenze, via Gino Capponi 9, I-50121 Florence, Italy*
[c] *Dipartimento di Chimica Generale ed Inorganica, Chimica Analitica e Chimica Fisica, Università di Parma, Centro di Studio per la Strutturistica Diffrattometrica del CNR, Parma, Viale delle Scienze 78, I-43100 Parma, Italy*

Received 23 December 1994

Abstract

The structures of the $[\{Ru(CO)_2(\mu\text{-}OOCCH_3)L\}_2]$ with $L = P^nBu_3$, P^tBu_3 or P^iPr_3 have been determined and their catalytic activity tested in the hydrogenation of internal and terminal olefins, of the carbonyl double bond and of both free and esterified carboxylic groups. There is a correlation between the P–Ru–Ru–P torsion angle and the catalytic activity of the complex.

Keywords: Ruthenium; Carboxylate complexes; Phosphine complexes; Catalysis; X-ray structures

1. Introduction

Several phosphine-substituted ruthenium carbonyl carboxylates have been synthesized and tested as catalysts in homogeneous hydrogenation [1–7], isomerization [8] and oligomerization [9] of unsaturated organic substrates.

Recently, we found that a catalytic precursor of the type $[\{Ru(CO)_2(\mu\text{-}OOCCH_3)L\}_2]$ provides different results for $L = P^nBu_3$, P^tBu_3, P^iPr_3 for the hydrogenation of dimethyl oxalate to methyl glycolate and ethylene glycol [7].

We have determined the X-ray structures of the above complexes in order to detect correlations between the structure of the complex, the type of substituent introduced and its catalytic activity. The electronic and steric influence of a ligand in a complex [10–16] may induce structural changes affecting its catalytic activity for particular reactions [17,18]. The IR spectra of the above complexes [7,19] are the same both in the solid state and in solution.

2. Results and discussion

2.1. Synthetic methods

The complexes $[\{Ru(CO)_2(\mu\text{-}OOCCH_3)(P^iPr_3)\}_2]$ **(I)** [7], $[\{Ru(CO)_2(\mu\text{-}OOCCH_3)(P^tBu_3)\}_2]$ **(II)** [7] and $[\{Ru(CO)_2(\mu\text{-}OOCCH_3)(P^nBu_3)\}_2]$ **(III)** [19] were synthesized as reported.

2.2. Structures of compounds I, II and III

The atomic coordinates of compounds **I–III** are given in Table 1 and the relevant parameters describing their molecular structures are compared in Table 2. The crystals of the three compounds consist of discrete neutral dinuclear molecules whose structures are similar to those of the analogous $[\{Ru(CO)_2(\mu\text{-}OOCCH_3)(PH^tBu_2)\}_2]$ **(IV)** [20], $[\{Ru(CO)_2(\mu\text{-}OOC(CH_2)_2CH_3)(P^tBu_3)\}_2]$ **(V)** [21], $[\{Ru_2(CO)_4(\mu\text{-}OOCCH_3)_2(P^nBu_3)\}_2]$ **(VI)** [22] and $[\{Ru_2(CO)_4(\mu\text{-}OOC(CH_2)_3COO)(P^nBu_3)_2\}_2]$ **(VII)** [22] where two octahedrally coordinated ruthenium atoms are joined by a direct Ru–Ru interaction and two *cis* bridging carboxylates as shown in Fig. 1. The coordination about each metal

* Corresponding author.

SSDI 0022-328X(95)05518-5

Table 1
Final fractional atomic coordinates ($\times 10^4$), with e.s.d.s in parentheses

Atom	X/a	Y/b	Z/c
$C_{26}H_{48}O_8P_2Ru_2$ (I)			
Ru1	1868.9(3)	955.2(5)	2841.7(3)
Ru2	2807.9(3)	−616.5(5)	2226.5(3)
P1	1171(1)	2143(2)	3717(1)
P2	3745(1)	−2135(2)	2000(1)
O1	1503(3)	−539(4)	3434(3)
O2	2463(3)	−1691(4)	3144(3)
O3	2813(3)	1017(5)	3765(3)
O4	3652(3)	32(5)	3138(3)
O10	622(3)	695(5)	1478(3)
O11	2448(4)	2931(5)	1956(4)
O21	1545(4)	−1483(5)	1019(3)
O22	3164(4)	1078(6)	998(4)
C1	1887(4)	−1457(7)	3492(4)
C2	1639(5)	−2370(8)	4040(5)
C3	3471(4)	574(7)	3718(4)
C4	4089(5)	743(10)	4403(5)
C11	2223(4)	2174(7)	2302(5)
C12	1095(4)	791(6)	2012(4)
C21	2031(4)	−1148(7)	1491(5)
C22	3049(4)	428(7)	1475(5)
C11P	266(5)	2814(7)	3225(5)
C12P	−354(5)	1911(9)	2969(5)
C13P	421(5)	3572(8)	2528(6)
C21P	837(5)	1270(7)	4518(4)
C22P	239(6)	1832(9)	4984(6)
C23P	1513(6)	722(8)	5071(5)
C31P	1733(6)	3336(7)	4232(5)
C32P	2378(7)	3819(10)	3850(7)
C33P	1228(7)	4309 (9)	4517(7)
C41P	4140(6)	−2020(10)	1040(6)
C42P	3454(7)	−2062(16)	380(7)
C43P	4645(7)	−943(12)	987(8)
C51P	4639(5)	−2076(8)	2737(6)
C52P	5386(6)	−2683(10)	2540(7)
C53P	4476(6)	−2409(12)	3555(6)
C61P	3381(7)	−3652(8)	2102(8)
C62P	2534(6)	−3843(9)	1872(8)
C63P	3856(8)	−4592(11)	1723(13)
$C_{32}H_{60}O_8P_2Ru_2$ (II)			
Ru1	887.5(3)	4139.7(2)	7861.4(1)
Ru2	−710.1(3)	5981.2(2)	7096.3(1)
P1	1773.1(10)	2288.4(7)	8646.7(5)
P2	−2786.7(10)	7414.0(7)	6349.0(6)
O11	3630(3)	4224(3)	6779(2)
O12	2374(3)	5349(2)	8907(2)
O21	921(3)	7329(2)	7959(2)
O22	1776(3)	6052(2)	5853(2)
O4	−1797(3)	4875(2)	6607(1)
O3	−195(3)	3411(2)	7040(1)
O1	−1228(3)	4240(2)	8522(1)
O2	−2281(3)	5889(2)	8072(1)
C11	2577(4)	4169(3)	7202(2)
C12	1776(4)	4876(3)	8519(2)
C21	265(4)	6826(3)	7613(2)
C22	792(4)	6015(3)	6318(2)
C1	−2270(3)	5065(3)	8513(2)
C2	−3639(4)	5056(3)	9087(2)
C3	−1335(4)	3891(3)	6661(2)
C4	−2222(4)	3235(3)	6235(2)

Table 1 (continued)

Atom	X/a	Y/b	Z/c
C11P	4000(4)	1884(3)	8650(3)
C12P	4699(5)	2059(6)	7841(4)
C13P	4587(5)	2601(4)	9192(5)
C14P	4670(5)	742(4)	8933(3)
C21P	1018(4)	2304(3)	9731(2)
C22P	1060(5)	3382(3)	10027(2)
C23P	−678(5)	2229(4)	9804(3)
C24P	1879(6)	1414(4)	10298(3)
C31P	1039(4)	1170(3)	8203(2)
C32P	1808(6)	1037(4)	7384(3)
C33P	−714(5)	1506(3)	8109(3)
C34P	1342(6)	73(3)	8662(3)
C41P	−2171(6)	8764(3)	6227(4)
C42P	−1656(9)	9034(4)	7020(5)
C43P	−779(7)	8693(4)	5658(5)
C44P	−3377(7)	9738(4)	5934(4)
C51P	−3100(4)	7023(3)	5311(2)
C52P	−1537(5)	6471(4)	4963(2)
C53P	−3807(5)	7952(4)	4738(3)
C54P	−4137(5)	6205(4)	5351(3)
C61P	−4771(4)	7609(4)	6882(3)
C62P	−6120(5)	8315(4)	6431(3)
C63P	−4659(7)	8126(5)	7658(3)
C64P	−5192(4)	6531(4)	7106(3)
$C_{32}H_{60}O_8P_2Ru_2$ (III)			
Ru1	2087(3)	893(2)	2056(2)
Ru2	2965(3)	−159(2)	3137(2)
P1	1272(9)	1577(7)	924(7)
P2	3698(9)	−1287(7)	3836(7)
O1	1983(18)	−912(18)	2710(17)
O2	1197(17)	−130(21)	1918(16)
O3	2738(21)	232(22)	1187(16)
O4	3462(24)	−557(17)	2085(18)
O11	1174(34)	1753(24)	3292(22)
O12	3417(27)	2119(21)	2255(19)
O21	4387(21)	988(19)	3650(17)
O22	2062(22)	417(23)	4512(21)
C1	1335(37)	−826(35)	2265(32)
C2	617(29)	−1385(28)	1880(26)
C3	3227(31)	−323(30)	1439(35)
C4	3595(24)	−760(23)	653(21)
C11	1491(36)	1399(35)	2838(34)
C12	2933(54)	1624(52)	2282(49)
C21	3770(32)	470(29)	3444(28)
C22	2451(34)	157(33)	4003(31)
C11P	1134(26)	2673(24)	1127(23)
C12P	564(38)	3143(39)	489(34)
C13P	199(48)	4032(52)	682(48)
C14P	495(48)	4408(45)	1303(47)
C21P	1726(29)	1551(26)	−95(25)
C22P	2640(31)	1912(30)	−32(28)
C23P	3070(37)	1660(33)	−856(32)
C24P	3954(37)	1879(33)	−791(31)
C31P	225(26)	1204(24)	595(24)
C32P	−346(29)	1210(25)	1235(26)
C33P	−1210(38)	750(34)	1006(34)
C34P	−1822(47)	748(43)	1624(41)
C41	3651(27)	−2164(25)	3208(24)
C42	4145(28)	−2957(28)	3679(26)
C43	4204(32)	−3635(31)	3042(28)
C44	4795(31)	−4392(28)	3453(27)
C51	4830(25)	−1147(23)	4216(23)

Table 1 (continued)

Atom	X/a	Y/b	Z/c
C52	5369(27)	−1055(25)	3507(24)
C53	6348(38)	−786(34)	3779(32)
C54	6924(36)	−634(33)	3110(32)
C61	3352(29)	−1610(26)	4887(25)
C62	2399(30)	−1856(29)	4693(28)
C63	2117(50)	−2167(51)	5602(51)
C64	1978(50)	−1631(53)	6144(49)

atom is completed by two *cis* terminal carbonyls and a terminal phosphine. The overall geometry of these molecules can be described as a "sawhorse-like" structure.

From Table 2, the Ru–P and P–C distances can be subdivided into two groups: the shortest values (Ru–P = 2.421(19) Å av., P–C = 1.859(4) Å av.) are found in compounds **I**, **III**, **IV**, **VI** and **VII** and the longest (Ru–P = 2.622(2) Å av., P–C = 1.928(8) Å av.) in compounds **II** and **V**. This is probably due to steric effects caused by the P^tBu_3 which is bulkier than the other phosphines. There are no significant differences in any of the seven compounds for the other distances.

The "sawhorse" shape shows a twist that is small in compounds **I**, **III**, **IV**, **VI** and **VII** (P–Ru–Ru–P is in the range 2.4–8.1°) and much greater in compounds **II** (P–Ru–Ru–P = 21.9°) and **V** (P–Ru–Ru–P = 58.2°). This twist is probably caused by steric effects involving the phosphines and the carboxylate groups. The last groups do not have the same conformation in these compounds, as indicated by the puckering analysis of the Ru–O–C–O–Ru rings shown in Table 3. These rings can be subdivided by the total puckering amplitudes [23] into two groups. The lowest puckering includes the PH^tBu_2 and P^nBu_3 derivatives and the highest puckering is observed in the butyrate compound.

The orientation of the phosphines is clearly illustrated by the Newman projections of Fig. 2, which show that it is similar in the cases of the *iso*propyl and *tert*-butyl derivatives (compounds **I**, **II** and **V**) with a P–C bond staggered between an Ru–O and an Ru–C bond, with the other two P–C bonds nearly eclipsed with respect to an Ru–O bond. In the case of the *n*-butylphosphine derivatives for P(1) of compound **III**, and all the phosphines of compounds **VI** and **VII**, the approximate eclipse is with two Ru–O bonds, whereas

Table 2
Comparison of average bond distances (Å) and angles (°), with e.s.d.s in parentheses

Bond	I	II	III	IV	V	VI	VII	Av.
Ru–Ru	2.738(1)	2.760(1)	2.718(5)	2.734(2)	2.728(1)	2.682(2)	2.734(3)	2.737(8)
Ru–O	2.138(4)	2.116(2)	2.096(34)	2.110(5)	2.134(5)	2.134(14)	2.135(5)	2.122(4)
Ru–C	1.837(4)	1.825(3)	1.757(47)	1.804(8)	1.826(9)	1.828(4)	1.854(8)	1.829(4)
Ru–P	2.458(2)	2.622(2)	2.393(9)	2.461(3)	2.622(4)	2.379(2)	2.396(3)	2.421(19)–2.622(2) [a]
P–C	1.860(5)	1.921(5)	1.831(28)	1.870(14)	1.938(6)	1.839(28)	1.857(6)	1.859(4)–1.928(8) [a]
C–O(carbonyl)	1.153(5)	1.153(2)	1.193(47)	1.162(9)	1.156(3)	1.150(5)	1.130(8)	1.153(2)
C–O(carboxyl)	1.255(5)	1.248(2)	1.206(30)	1.249(8)	1.254(16)	1.250(5)	1.242(8)	1.249(2)
C–C(phosph.)	1.525(6)	1.512(4)	1.537(23)	1.514(13)	1.537(6)	1.515(10)	1.549(13)	1.538(3)
C–C(carboxyl)	1.503(8)	1.527(3)	1.581(56)	1.504(13)	1.534(8)	1.521(9)	1.530(15)	1.524(4)
Ru–Ru–O	82.6(1)	82.0(2)	82.0(4)	82.7(3)	82.0(4)	84.0(10)	83.0(2)	82.5(1)
Ru–Ru–C	93.0(4)	93.6(6)	94.8(12)	93.5(3)	89.9(11)	95.3(17)	94.3(4)	93.5(3)
Ru–Ru–P	165.9(7)	165.1(9)	167.7(4)	162.1(2)	167.2(2)	165.7(1)	166.6(1)	165.9(6)
O–Ru–O	84.8(7)	85.7(5)	82.9(8)	82.8(3)	85.4(1)	83.8(2)	83.6(2)	84.7(4)
C–Ru–C	87.1(3)	86.8(1)	88.5(19)	87.7(7)	88.2(1)	88.1(6)	88.0(7)	87.5(3)
P–Ru–O	87.1(6)	88.0(16)	88.9(7)	84.0(3)	89.2(22)	87.5(10)	87.1(6)	85.6(8)
P–Ru–C	97.2(9)	97.4(19)	94.0(12)	98.6(3)	100.1(23)	93.0(2)	95.2(6)	94.9(10)
O–Ru–C(*cis*)	93.9(4)	93.5(15)	94.1(10)	94.1(7)	92.7(37)	94.0(3)	94.1(3)	94.0(2)
O–Ru–C(*trans*)	175.4(5)	174.1(5)	175.6(13)	175.5(9)	169.9(10)	177.4(2)	176.5(4)	176.5(6)
Ru–P–C	113.7(7)	111.8(2)	115.4(12)	118.8(6)	112.2(6)	114.4(5)	114.5(8)	112.9(8)
O–C–O	125.7(6)	125.2(4)	125.3(75)	123.6(8)	126.0(16)	125.9(5)	126.5(8)	125.4(3)
C–C–O	117.1(4)	117.4(2)	115.4(62)	118.1(8)	117.5(10)	117.0(8)	116.7(7)	117.3(1)
P–Ru–Ru–P phosphine	2.5(7)	21.9(9)	8.1(27)	2.4(6)	58.2(5)	7.8(6) [b]	6.6(12)	
Eff. cone angle [c]	138	139	144 –150	136	139	147	143	

(I) $[Ru(CO)_2(\mu\text{-}OOCCH_3)(P^iPr_3)]_2$; **(II)** $[Ru(CO)_2(\mu\text{-}OOCCH_3)(P^tBu_3)]_2$; **(III)** $[Ru(CO)_2(\mu\text{-}OOCCH_3)(P^nBu_3)]_2$; **(IV)** $[Ru(CO)_2(\mu\text{-}OOCCH_3)(PH^tBu_2)]_2$ [11]; **(V)** $[Ru(CO)_2(\mu\text{-}OOC(CH_2)_2CH_3)(P^tBu_3)]_2$ [21]; **(VI)** $[Ru_2(CO)_4(\mu\text{-}OOCCH_3)(P^nBu_3)]_2$ [22]; **(VII)** $[Ru_2(CO)_4(\mu\text{-}OOC(CH_2)_3COO\text{-}\mu)(P^nBu_3)]_2$ [22].

[a] See text.

[b] The bone of half-molecule is P–Ru–Ru–O, the molecule being a dimer with a bridging carboxylate.

[c] Calculated as twice the angle formed by Ru–P direction and the tangent from Ru to the most external hydrogen-atom sphere to which a van der Waals radius of 1.20 Å has been attributed.

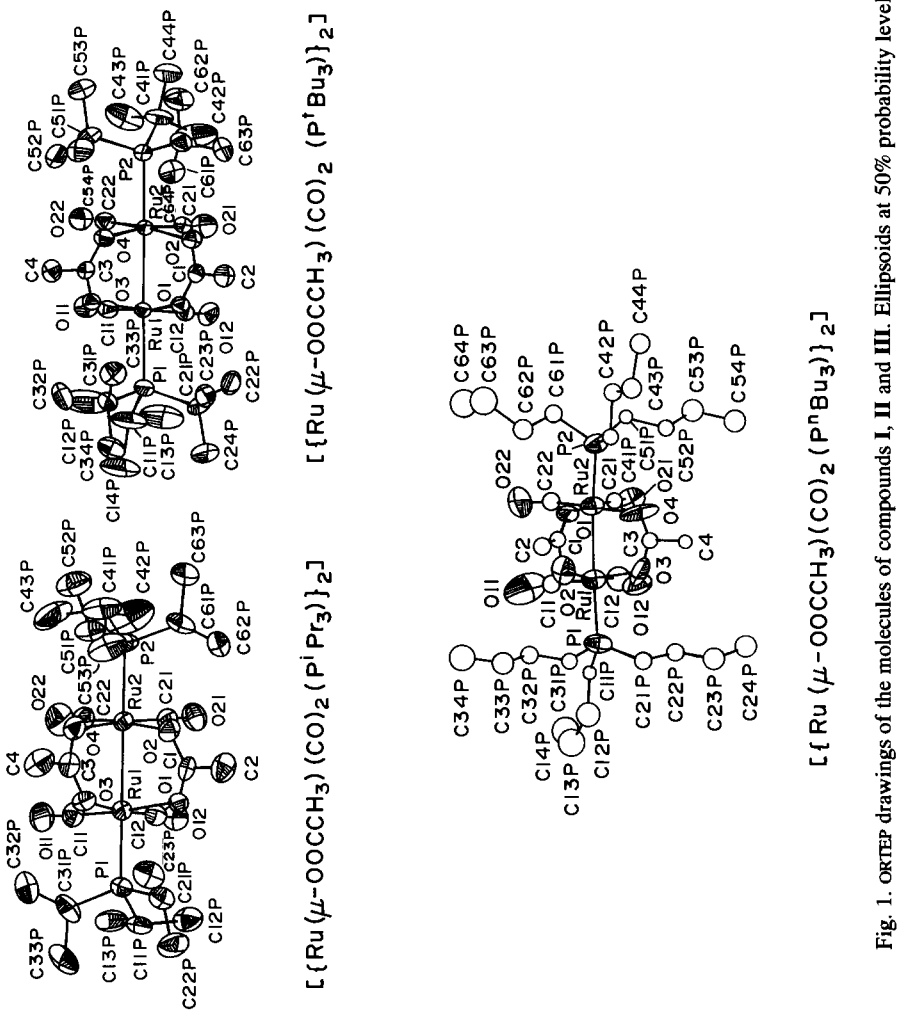

Fig. 1. ORTEP drawings of the molecules of compounds I, II and III. Ellipsoids at 50% probability level.

for P(2) of compound **III** it involves the two Ru–C bonds. For the di-*tert*-butylphosphine derivative (**IV**) all the P–C bonds are approximately staggered with the P–H bond projecting between two Ru–O bonds.

A better understanding of the conformations of the phosphines in these compounds is obtained from the van der Waals potential energy profiles in Fig. 3, which were calculated considering free molecules and positive values of the rotation angle ϕ corresponding to counter-clockwise rotations. The $\phi = 0°$ value is for the conformation found in the crystal and the energy values are relative to the energy corresponding to that conformation. From Fig. 3, it appears that the lowest energy barriers are found for the *n*-butylphosphines of compound **III** whose alkyl chains tend to be unfolded and spread parallel to the $RuO_2(CO)_2$ plane (Figs. 1 and 4), wherein the highest barriers are present in the di-*tert*-butylphosphine derivative (**IV**) where the two very high peaks at $\phi \approx \pm 110°$ are indicative of a situation leaving no room for rotation of the phosphine. Low barriers are observed also for the *n*-butylphosphines of the dimeric compounds **VI** and **VII**, except for the P(1) phosphine of compound **VII**, which gives two very high barriers of rotation at $\phi \approx -100°$ and 70° (Fig. 3), due to steric hinderance between the terminal methyls of the phosphine and a carboxyl oxygen, O(7), belonging to the adjacent di-metal moiety of the dimer. The peaks in the curves of Fig. 3 are due mainly to steric hindrance

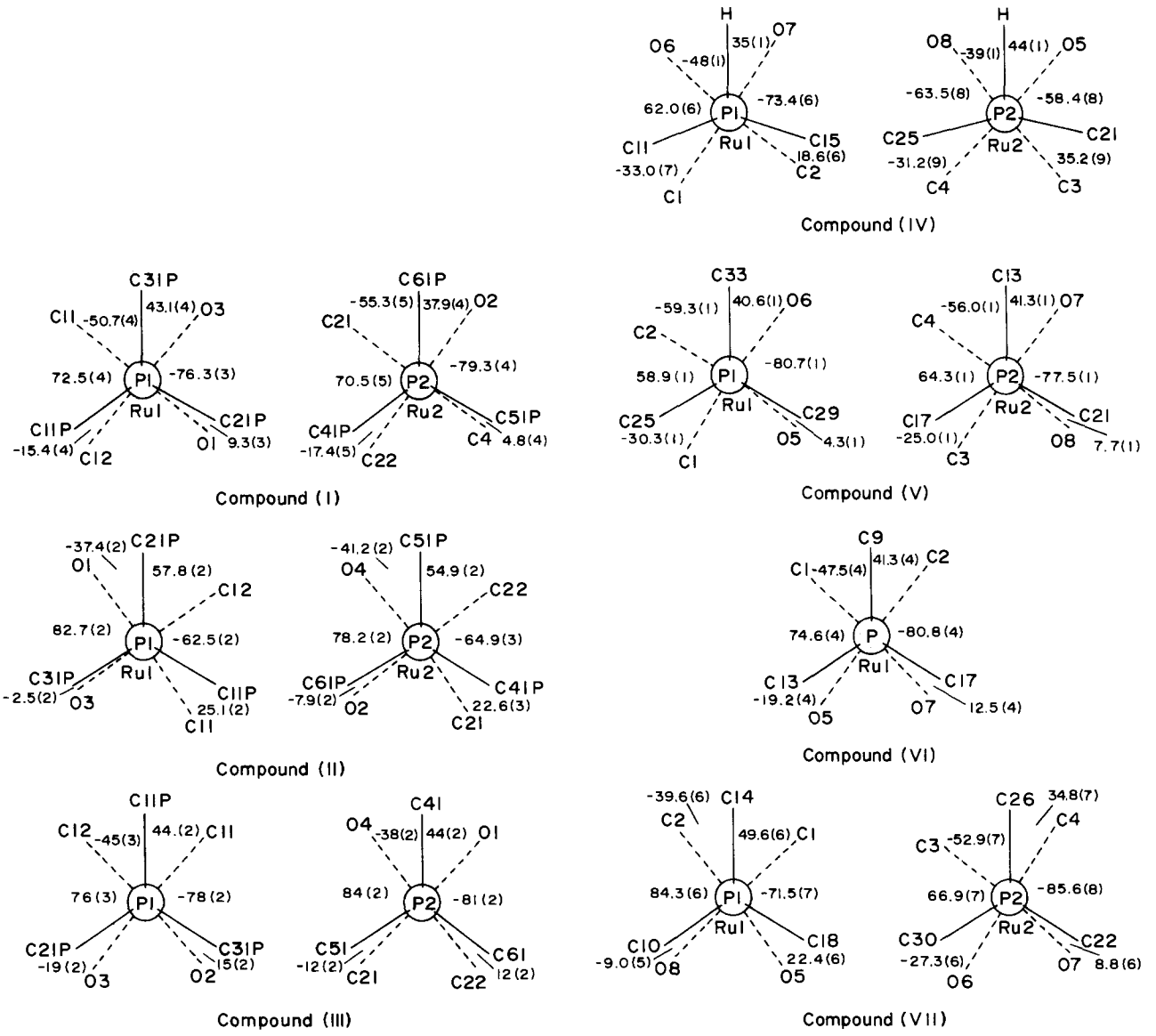

Fig. 2. Newman projections along the P–Ru bonds showing the orientations of the phosphine with respect to the Ru–C and Ru–O bonds.

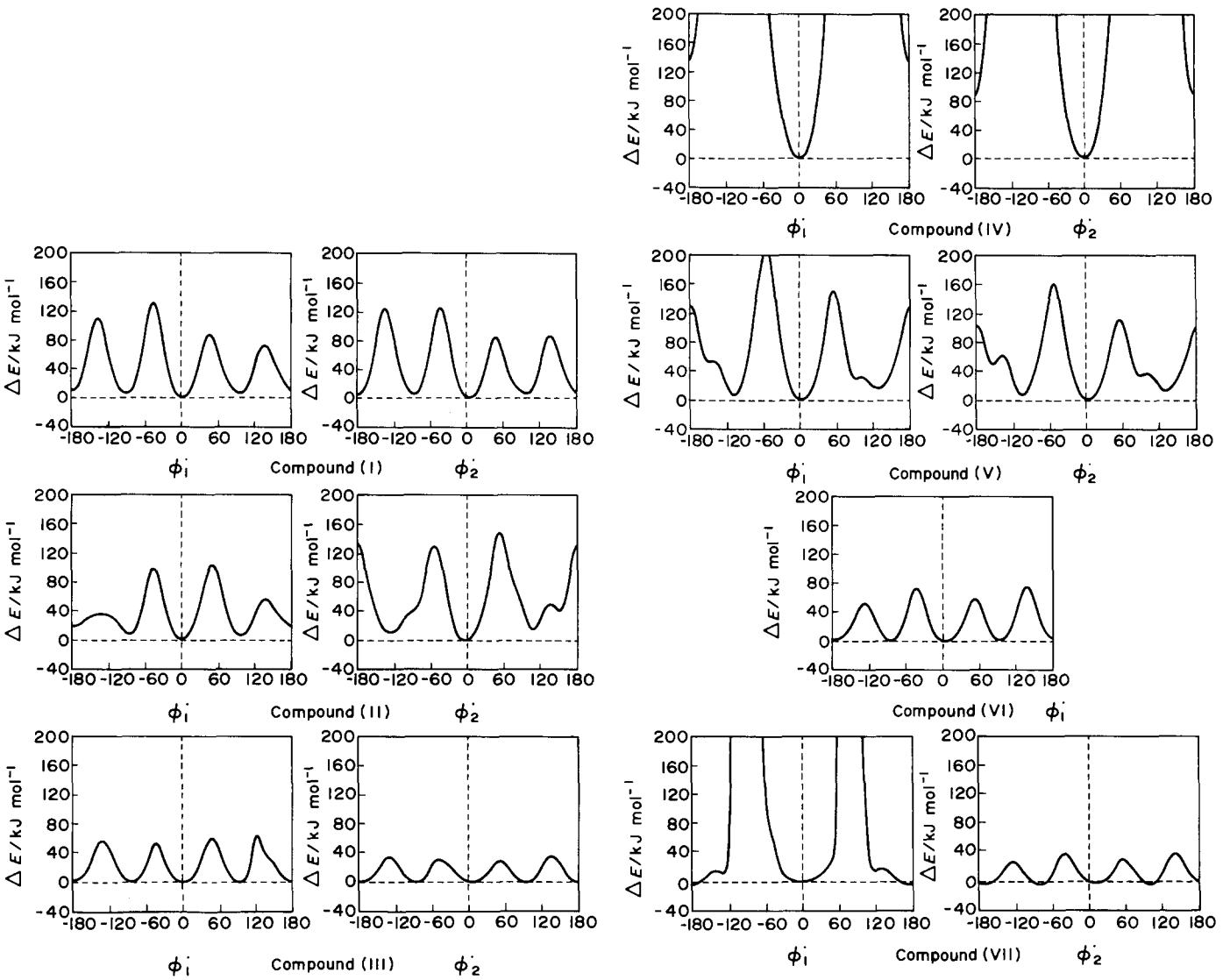

Fig. 3. Calculated difference potential energy profiles for rotation of the phosphines about Ru–P bonds; ϕ_1 and ϕ_2 refer to rotations about Ru(1)–P(1) and Ru(2)–P(2) bonds, respectively.

during rotation between the hydrogen atoms of the alkyls and the acetate and carbonyl oxygen. The alkyl chains of the tri-*n*-butylphosphine derivative are equally spread in the two independent ligands, as can be seen from the values of the effective cone angles, which are 150° for P(1) and 144° for P(2).

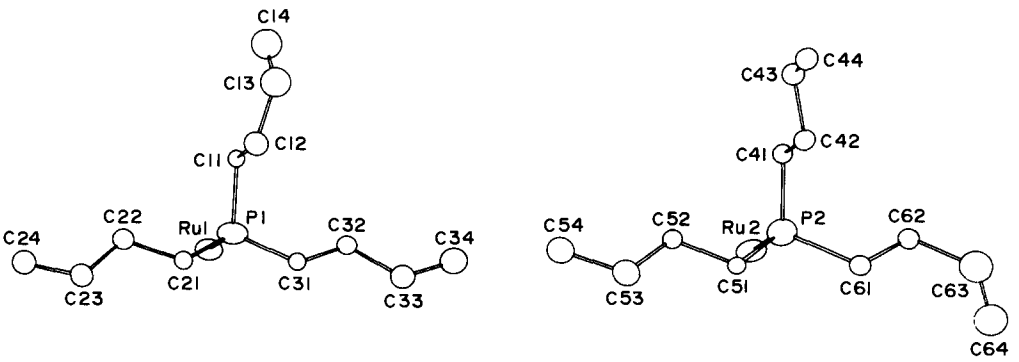

Fig. 4. Structures of the phosphine ligands in compound **III**, projected in planes approximately perpendicular to the Ru–P bonds, showing their extended conformation.

Table 3
Puckering parameters and conformation of the Ru–O–C–O–Ru rings

Compound	Ring [a]	Q_T [b]	*ADP* [c]	Conformation [d]
I	A	0.283(4)	Δ_2C(1) = 0.0002(13)	H–C
	B	0.255(5)	Δ_SRu(2) = 0.0236(31)	T
			Δ_2C(3) = 0.0248(23)	
II	A	0.263(3)	Δ_2C(1) = 0.0062(16)	H–C
	B	0.241(3)	Δ_2C(3) = 0.0185(15)	H–C
III	A	0.082(22)	Δ_2C(1) = 0.0028(150)	H–C
	B	0.060(35)	Δ_2O(3) = 0.0063(131)	T
			Δ_SO(4) = 0.0086(144)	
IV	A′	0.070(8)	Δ_2O(6) = 0.0056(30)	H–C
	B′	0.081(10)	Δ_SO(7) = 0.0072(40)	E
V	A″	0.385(1)	Δ_2C(5) = 0.0051(5)	H–C
	B″	0.383(2)	Δ_2C(9) = 0.0015(6)	H–C
VI	A‴	0.151(5)	Δ_2C(5) = 0.0133(22)	T
	B‴	0.136(4)	Δ_SRu(1) = 0.0147(30)	H–C
VII	A‴	0.101(7)	Δ_2O(6) = 0.0072(27)	H–C
	B⁗	0.088(7)	Δ_2C(9) = 0.0066(33)	T
			Δ_SRu(2) = 0.0099(46)	

[a] A = Ru(1)–O(1)–C(1)–O(2)–Ru(2); B = Ru(1)–O(3)–C(3)–O(4)–Ru(2); A′ = Ru(1)–O(6)–C(5)–O(5)–Ru(2); B′ = Ru(1)–O(7)–C(7)–O(8)–Ru(2); A″ = Ru(1)–O(6)–C(5)–O(8)–Ru(2); B″ = Ru(1)–O(5)–C(9)–O(7)–Ru(2); A‴ = Ru(1)–O(5)–C(5)–O(6)–Ru(2); B‴ = Ru(1)–O(7)–C(7)–O(8)–Ru(2); B⁗ = Ru(1)–O(8)–C(9)–O(7)–Ru(2).
[b] Q_T = total puckering amplitude [23].
[c] *ADP* = asymmetry displacement parameters [24].
[d] H-C = half-chair; E = envelope; T = twisted.

2.3. Catalytic activity

The catalytic activity of **I**, **II** and **III** was tested in the reduction of internal and terminal olefins, of the carbonyl double bond and of both free and esterified carboxylic groups.

Reactions were performed in toluene at 120°C, under 130 atm of dihydrogen (Table 4). Olefins are easily hydrogenated, especially if they are terminal. Carbonyl groups are also rapidly hydrogenated to alcohols (cyclohexanone at a higher rate than acetone), whereas the hydrogenation of a carboxylate is more difficult. In the reduction of dimethyl oxalate with the tri-*tert*-butylphosphine-substituted precursor, the hydrogenolysis of the substrate to methyl formate, methane and carbon dioxide is competitive with that leading to methyl glycolate.

Table 5
Steric, electronic and spectroscopic characteristics of the trialkylphosphines

Parameter	P^tBu_3	P^iPr_3	P^nBu_3
pK_a [12]	11.40	–	8.43
^{31}P NMR shift (ppm)	−63.3 [11]	−20.0 [11]	32.7 [16]
χ [12]	0	3.45	5.25

With all substrates examined, the catalytic activity of the three complexes depends on the phosphine, decreasing in the order $P^tBu_3 > P^nBu_3 > P^iPr_3$. This is not consistent with the literature [11,17,18] where correlations are made with the electronic and/or steric characteristics of the substituents in the catalytically active species. Both steric and electronic properties of the phosphines (Table 5) suggest an order $P^tBu_3 > P^iPr_3 > P^nBu_3$ which involves the inversion of P^iPr_3 and P^nBu_3 with respect to the reactivity data found. However, the role of the catalyst is to activate the reagents, which in our reactions involves not only the organic substrate but also molecular hydrogen.

In order to obtain more detailed information on the activation of the olefin by the catalytic system $[\{Ru(CO)_2(\mu\text{-}OOCCH_3)L\}_2]$, we investigated the isomerization of hex-1-ene in the absence of dihydrogen (Table 6). The conversions obtained in this isomerization are in the same sequence as in the hydrogenation. The isomeric composition of the olefins seems very near the equilibrium composition in the experiments with the more active catalysts, which appeared to be those with the *tert*-butyl and *n*-butyl phosphines. The activation of the olefin, the only activation step in the isomerization reactions, therefore seems to be the rate-determining step both in the isomerization and in the hydrogenation reactions. At the end of isomerization tests, the catalyst precursors were recovered unaltered.

The ease of access of the substrate to the metal atom,

Table 4
Hydrogenation of various substrates in the presence of complexes $[\{Ru(CO)_2(\mu\text{-}OOCCH_3)L\}_2]$

Substrate	Time (h)	Product	Conversion (%)		
			L = P^tBu_3	L = P^nBu_3	L = P^iPr_3
Isobutene [a]	15	Isobutane	78.5	41.8	37.9
Cyclohexene	1	Cyclohexane	97.0	47.9	41.3
Acetone	6	Propan-2-ol	23.0	21.7	7.3
Cyclohexanone	6	Cyclohexanol	79.2	70.8	52.1
Dimethyl oxalate	72	Methyl glycolate	2.1 [b]	31.3	16.5
Acetic acid	72	Ethyl acetate	5.0	4.6	4.2

Conditions: $p(H_2)$ = 130 atm; cat = 0.036 mmol; substrate = 0.011 mol; toluene = 10 ml; T = 120°C. Catalyst precursors were recovered unaltered from the crudes except in the hydrogenation of dimethyl oxalate carried out in the presence of the P^tBu_3 derivative.
[a] T = 60°C.
[b] Also 15% conversion to $HCOOCH_3$, CH_4 and CO_2.

Table 6
Isomerization of hex-1-ene to hex-2- and -3-ene in the presence of complexes [{Ru(CO)$_2$(μ-OOCCH$_3$)L}$_2$]

L	Conversion (%)	Composition of reaction products (%)			
		trans-2-ene	*cis*-2-ene	*trans*-3-ene	*cis*-3-ene
P^{t}Bu$_3$	42.4	70.5	20.8	7.5	1.2
P^{n}Bu$_3$	34.2	71.6	19.6	7.0	1.8
P^{i}Pr$_3$	7.4	50.0	35.2	6.7	8.1

Conditions: p(N$_2$) = 1 atm; cat. = 0.036 mmol; substrate = 0.011 mol; toluene = 10 ml; T = 100°C; reaction time = 15 h.

the "core" of the complex relevant in determining the activity of the catalyst, is connected with its structure. A coordinatively unsaturated site must be formed, probably by an initially bidentate acetate becoming monodentate. However, the structural data of our complexes show that bond lengths and angles do not parallel the sequence P^{t}Bu$_3$ > P^{n}Bu$_3$ > P^{i}Pr$_3$ observed in the catalytic tests (Tables 4 and 6). The only structural parameter that seems to be related to the observed reactivity is the P–Ru–Ru–P torsion angle (Table 2) which, being a

Table 7
Experimental data for crystallographic analyses

	I	II	III
Formula	$C_{26}H_{48}O_8P_2Ru_2$	$C_{32}H_{60}O_8P_2Ru_2$	$C_{32}H_{60}O_8P_2Ru_2$
Molecular weight	752.8	836.9	836.9
Space group	$P2_1/c$	$P\bar{1}$	$P2_1/c$
a (Å)	17.337(11)	8.812(2)	15.582(10)
b (Å)	11.559(7)	12.816(6)	16.377(10)
c (Å)	17.133(10)	17.098(15)	16.370(6)
α (°)	–	85.25(1)	–
β (°)	97.30(2)	86.97(7)	96.86(4)
γ (°)	–	78.44(1)	–
V (Å^3)	3406(4)	1884(2)	4148(4)
Z	4	2	4
D_c (mg m^{-3})	1.468	1.475	1.340
Reflection for number	26	25	24
Lattice parameters θ range (°)	19/24	11/17	8/14
Radiation	Mo Kα_1	Mo Kα_1	Mo Kα_1
Crystal data			
Wavelength (Å)	0.709300	0.709300	0.709300
F(000)	1544	868	1736
Crystal size (mm)	0.21 × 0.34 × 0.40	0.33 × 0.37 × 0.41	0.09 × 0.21 × 0.32
Diffractometer	Philips PW 1100	CAD-4	CAD-4
μ (mm^{-1})	1.001	0.912	0.829
Absorption correction (min., max.)	0.94695–1.095623	–	–
Scan speed (° min^{-1})	0.75	3.30	3.30
Scan width (°)	1.60	0.80 + 0.35 tan θ	0.80 + 0.35 tan θ
Radiation for intensity measurements	Mo Kα	Mo Kα	Mo Kα
θ range (°)	3–25	3–25	3–18
h range	−20/20	−10/10	−13/13
k range	0/13	−15/15	0/14
l range	0/20	0/20	0/14
Standard reflection	406	2$\bar{7}$6	451
Intensity variation	None	None	None
Scan mode	$\omega - 2\theta$	$\omega - 2\theta$	$\omega - 2\theta$
No. of measured reflections	6013	6942	3121
Condition for observed reflection	$I > 2\sigma(I)$	$I > 2\sigma(I)$	$I > 2\sigma(I)$
No. of reflections used in the refinement	3994	4916	1109
$R_{int} = \Sigma(I - \langle I \rangle)/\Sigma I$	0.0268	0.0097	0.07
Anisotropic least-squares on F	Block diagonal	Full matrix	Full matrix
Max. L.-S. shift to error ratio	0.267 (non H)	0.143	0.049
Min., max. height in final $\Delta\rho$/(e Å^{-3})	−0.16/0.13	−0.20/0.20	−0.25/0.46
No. of refined parameters	536	619	237
$R = \Sigma \mid \Delta F \mid / \Sigma \mid F_o \mid$	0.0496	0.0251	0.0749
$R_w = [\Sigma w(\Delta F)^2 / \Sigma w F_o^2]^{1/2}$	0.0545	0.0359	0.0863
$S = [\Sigma w(\Delta F)^2/(N-P)]^{1/2}$ [a]	1.3227	0.9042	8.5205
k, g $\{w = k[\sigma^2(F_o) + gF_o^2]\}$	1.5401, 0.0005	0.1920, 0.005	$w = 1$

[a] P = number of parameters, N = number of observations.

measure of the distortion of the central binuclear "core" of the complex with respect to the phosphines, drops from the most hindered ligand P^tBu_3 to the more flexible P^nBu_3 and the less crowded P^iPr_3 derivatives. It may be that the larger the distortion, the easier is the access of the substrate molecules to the metal atom responsible for their activation and reactivity. Nevertheless, the difference between the P–Ru–Ru–P torsion angles for the complexes of P^nBu_3 and P^iPr_3 is much less than that for the more crowded P^tBu_3 derivative.

The calculated difference potential energy profiles (Fig. 3), which are lower for the P^nBu_3 derivative than for the P^iPr_3 derivative, may explain the higher activity of the P^nBu_3-substituted catalyst, in spite of the disordered *n*-butyl chains, because of the greater freedom of rotation.

We cannot exclude that effects other than steric effects contribute to the observed reactivity.

3. Experimental

GLC analyses were performed on a Shimadzu GC-14A chromatograph; ^1H, ^{31}P and ^{13}C NMR spectra were recorded on a Varian FT 80A spectrometer operating at 79.5, 32.2 and 20.0 MHz, respectively; GLC mass spectra were recorded with a HP 5970A spectrometer; IR spectra were recorded using a Perkin-Elmer 580B data system; molecular weight determinations based on the isopiestic method were performed using a Wescam Model 233 instrument; elemental analyses were performed with a Perkin-Elmer 240C elemental analyser.

3.1. Materials

Isobutene, cyclohexene, acetone, cyclohexanone, dimethyl oxalate, acetic acid, hex-1-ene, tri-*n*-butylphosphine (P^nBu_3), tri-*tert*-butylphosphine (P^tBu_3) and tri*iso*propylphosphine (P^iPr_3) were commercial products.

3.2. Hydrogenation and isomerization experiments

The hydrogenation experiments were carried out as previously described [25]; the isomerization experiments were carried out in a 150 ml stainless-steel rocking autoclave under dinitrogen. The amounts of reactants and reaction conditions are reported in Tables 4 and 6.

3.3. Analytical procedures and identification of products

The residual gas from each experiment was monitored by IR spectroscopy. The conversions of isobutene, cyclohexene, acetone, cyclohexanone, acetic acid and hex-1-ene were determined by GLC analysis. The conversion of dimethyl oxalate was determined as previously reported [7]. All reaction products (isobutane, cyclohexane, propan-2-ol, cyclohexanol, methyl glycolate, ethyl acetate, *cis*- and *trans*-hex-2-ene and *cis*- and *trans*-hex-3-ene) were identified by their GLC mass spectra [26].

3.4. Preparation of complexes

$[\{Ru_2(CO)_4(\mu\text{-}OOCCH_3)_2\}_n]$ [19], $[\{Ru(CO)_2(\mu\text{-}OOCCH_3)(P^iPr_3)\}_2]$ (**I**) [7], $[\{Ru(CO)_2(\mu\text{-}OOCCH_3)(P^tBu_3)\}_2]$ (**II**) [7] and $[\{Ru(CO)_2(\mu\text{-}OOCCH_3)(P^nBu_3)\}_2]$ (**III**) [19] were prepared as previously reported.

3.5. Crystal structure analysis of compounds I, II and III

Table 7 summarizes the data for the crystal structure analyses. The lattice parameters were refined by a least-squares procedure [27] using the Nelson and Riley [28] extrapolation function. The intensities were measured at room temperature, 293 ± 2 K, and in no case were the intensity variations of the standard reflections greater than 0.2%. The individual reflection profiles were analysed using the method of Lehman and Larsen [29], the intensity data were corrected for Lorentz and polarization effects and the absorption was taken into account only for compound **I**, by the azimuthal-scan method [30].

The structures were solved by Patterson analysis of SHELX86 [31] and Fourier methods, and refined by least-squares on *F*, using the SHELX76 [32] program. In the case of compounds **I** and **II**, the non-hydrogen atoms were all refined anisotropically, whereas for compound **III** this treatment was applied only to the heaviest atoms, Ru, P and O, as the number of observed reflections was small owing to the small size of the sample. As a consequence, the results of the analysis of this compound cannot be considered very accurate, although they are good enough for a reliable discussion of the molecular geometry.

As frequently happens with hydrocarbon chains, disorder was found for the terminal methyls of some of the butyl chains, as indicated by the exceptionally high values of the anisotropic displacement parameters of these atoms (see also the ORTEP ellipsoids in Fig. 1). In spite of this disorder, and of the presence of the heavy ruthenium atoms, many hydrogen atoms were located in the final electron density difference maps for compounds **I** and **II**; for compound **III** these atoms were considered to be in calculated positions. For **I** and **II** the hydrogen atoms were refined isotropically but, at the end of the analysis for the geometrical calculations needed for the discussion of the structures, all the hydrogen atoms were considered in calculated positions.

The atom–atom potential energy calculations were carried out with the ROTENER program [33], which makes use of a function of the type $E_{ij} = B_{ij} \exp(-C_{ij} r_{ij}) - A_{ij} r_{ij}^{-6}$, to calculate the van der Waals non-bonded energy. In addition to the quoted programs, PARST [34], THMV [35] and ORTEP [36] were used.

Atomic scattering factors and anomalous scattering coefficients were taken from Ref. [37]. The crystallographic calculations were carried out on the ENCORE–POWERNODE 6040 computer of the Centro di Studio per la Strutturistica Diffrattometrica del CNR (Parma).

Additional material available from Cambridge Crystallographic Data Centre comprises H-atom coordinates, anisotropy atomic displacement parameters and remaining bond lengths and angles.

Throughout the paper the averaged values are means, weighted according to the reciprocals of the variances and the corresponding e.s.d.s are the largest of the values of the "external" and "internal" standard deviations [38].

Supplementary data are available.

Acknowledgements

This work was supported by a grant from MURST (40%) and CNR, Progetto Finalizzato per la Chimica Fine e Secondaria II.

References

[1] U. Matteoli, M. Bianchi, G. Menchi, P. Frediani and F. Piacenti, *J. Mol. Catal.*, *29* (1985) 269.
[2] U. Matteoli, G. Menchi, P. Frediani, M. Bianchi and F. Piacenti, *J. Organomet. Chem.*, *285* (1985) 281.
[3] U. Matteoli, G. Menchi, M. Bianchi, P. Frediani and F. Piacenti, *Gazz. Chim. Ital.*, *115* (1985) 603.
[4] U. Matteoli, G. Menchi, M. Bianchi and F. Piacenti, *J. Organomet. Chem.*, *299* (1986) 233.
[5] F. Piacenti, P. Frediani, U. Matteoli, G. Menchi and M. Bianchi, *Chim. Ind. (Milan)*, *68* (1986) 53.
[6] U. Matteoli, G. Menchi, M. Bianchi and F. Piacenti, *J. Mol. Catal.*, *44* (1988) 347.
[7] U. Matteoli, G. Menchi, M. Bianchi and F. Piacenti, *J. Mol. Catal.*, *64* (1991) 257.
[8] G. Menchi, U. Matteoli, A. Scrivanti, S. Paganelli and C. Botteghi, *J. Organomet. Chem.*, *354* (1988) 215.
[9] M. Bianchi, G. Menchi, U. Matteoli and F. Piacenti, *J. Organomet. Chem.*, *451* (1993) 139.
[10] T.L. Brown and K.J. Lee, *Coord. Chem. Rev.*, *128* (1993) 89.
[11] C.A. Tolman, *Chem. Rev.*, *77* (1977) 313.
[12] Md.M. Rahman, H. Ye Liu, K. Eriks, A. Prock and W.P. Giering, *Organometallics*, *8* (1989) 1.
[13] Md.M. Rahman, H. Ye Liu, A. Prock and W.P. Giering, *Organometallics*, *6* (1987) 650.
[14] T.T. Derencsényi, *Inorg. Chem.*, *20* (1981) 665.
[15] B.E. Mann and A. Musco, *J. Chem. Soc. Dalton Trans.*, (1980) 776.
[16] B.E. Mann, *J. Chem. Soc. Perkin Trans. 2*, (1972) 30.
[17] M. Tamura, M. Ishino, T. Deguchi and S. Nakamura, *J. Organomet. Chem.*, *312* (1986) C75.
[18] H.-O. Tanaka, Y. Hara, E. Watanabe, K. Wada and T. Onoda, *J. Organomet. Chem.*, *312* (1986) C71.
[19] G.R. Crooks, B.F.G. Johnson, J. Lewis, I.G. Williams and G. Gamlen, *J. Chem. Soc. A*, (1969) 2761.
[20] H. Schumann, J. Opitz and J. Pickardt, *J. Organomet. Chem.*, *128* (1977) 253.
[21] T.A. Bright, R.A. Jones and C.M. Nunn, *J. Coord. Chem.*, *18* (1988) 361.
[22] M. Bianchi, U. Matteoli, P. Frediani, F. Piacenti, M. Nardelli and G. Pelizzi, *Chim. Ind. (Milan)*, *63* (1981) 475.
[23] D. Cremer and J.A. Pople, *J. Am. Chem. Soc.*, *97* (1975) 1354.
[24] M. Nardelli, *Acta Crystallogr., Sect. C*, *39* (1983) 1141.
[25] M. Bianchi, G. Menchi, F. Francalanci, F. Piacenti, U. Matteoli, P. Frediani and C. Botteghi, *J. Organomet. Chem.*, *188* (1980) 109.
[26] S.R. Hellez and G.W.A. Milne, *EPA / NIH Mass Spectral Data Base*, Vol. 1, US Department of Commerce/National Bureau of Standards, Washington, DC, 1978.
[27] M. Nardelli and A. Mangia, *Ann. Chim (Rome)*, *74* (1984) 163.
[28] J.B. Nelson and D.P. Riley, *Proc. Phys. Soc. (London)*, *57* (1945) 160 and 447.
[29] M.S. Lehmann and F.K. Larsen, *Acta Crystallogr., Sect. A*, *30* (1974) 580.
[30] A.C.T. North, D.C. Phillips and F. Scott Mathews, *Acta Crystallogr., Sect. A*, *24* (1968) 351.
[31] G.M. Sheldrick, *SHELX86*, *Program for Crystal Structure Solution*, University of Göttingen, Göttingen, 1986.
[32] G.M. Sheldrick, *SHELX76*, *Program for Crystal Structure Determination*, University of Cambridge, Cambridge, 1976.
[33] M. Nardelli, *ROTENER*, *a FORTRAN Routine for Calculating Non-bonded Potential Energy*, University of Parma, Parma, 1988.
[34] M. Nardelli, *Comput. Chem.*, *7* (1983) 95.
[35] K.N. Trueblood, THMV, University of California, Los Angeles, 1984.
[36] C.K. Johnson, *ORTEP*, *Report ORNL-3794*, Oak Ridge National Laboratory, Oak Ridge, TN, 1965.
[37] *International Tables for X-ray Crystallography*, Vol. 4, Kynoch Press, Birmingham (present distributor Kluwer, Dordrecht), 1974, pp. 99 and 149.
[38] H. Topping, *Errors of Observation and Their Treatment*, Chapman and Hall, London, 1960, p. 91.